Journal of Materials Chemistry A

A robust, sustainable and multifunctional nanofiber with smart switch ability for water-in-oil and oil-in-water emulsions separation and liquid marble preparation

Journal:	*Journal of Materials Chemistry A*
Manuscript ID	TA-ART-09-2019-010320.R1
Article Type:	Paper
Date Submitted by the Author:	28-Oct-2019
Complete List of Authors:	Arshadi, Mohammad ; Cornell University, Food Science Azizi, Morteza; Cornell University Soozandeh, Hamid; Cornell University Tan, Chen; Cornell University College of Agriculture and Life Sciences Davachi, Seyed Mohammad; Cornell University, Abbaspourrad, Alireza; Cornell University, Food Science; Cornell University

A robust, sustainable and multifunctional nanofiber with smart switch ability for water-in-oil and oil-in-water emulsions separation and liquid marble preparation

Mohammad Arshadi, Morteza Azizi, Hamid Souzandeh, Chen Tan, Seyed Mohammad Davachi,

Alireza Abbaspourrad*

Department of Food Science, College of Agriculture and Life Sciences, Cornell University, 243 Stocking Hall, Ithaca, NY 14853, United States

Abstract

Various membranes have been developed for the separation of oil/water mixtures, however, their fabrication require toxic reagents, multiple processing steps, and advanced technologies. Nature not only precisely generates unique materials but also provides tremendous examples in the environment that can be used inspiration for the development and creation of smart and green materials. In this study, we prepare a multifunctional nanobiofiber (NBF) from grape seed in a one-pot reaction using green solvent that by making them into a smart layer, can switch between a state of underwater superoleophobic wetting to a state of underoil superhydrophobicity and back without using any external stimuli. The several μm length and 50 nm width of the NBF exhibits robust stability and provides a porous NBF layer, suggesting its potential for the simultaneous separation of various surfactant-stabilized water-in-oil and oil-in-water emulsions while showing a high dye adsorption from water (100% for methylene blue). Furthermore, by rolling the water droplets on the surface of the NBF powder, an effective microreactor, known as a liquid marble, is prepared for the first time using a bio-originated, superamphiphilic material in air, rather than hydrophilic or hydrophobic material, and can be used to remove dye within 30 s. Moreover, based

on the ability of NBFs to encapsulate a high volume of water (120 μL), we demonstrate another application of the NBF powder as an additive to soil for maintaining the soil moisture in arid conditions, allowing us to successfully demonstrate the growth of a lentil seed. This multi-functional, low-cost, and green NBF material shows excellent sustainability and mechanical/chemical stability for promising multiple environmental remediation implementation.

Introduction

The amount of energy consumed for the separation of chemicals is approaching ~10–15% of the world's total energy consumed pre year.[1] Furthermore, in recent years oil contamination from frequent spills and increasingly oily industrial sewage has become one of the most important issues that threatens the environment and water resources.

Several traditional methods like air flotation, flocculation, oil-absorbing materials, gravity separation combined with skimming, and coagulation, currently are using for oil/water separation and suffer from low separation performance, complicated separation steps and high-energy consumption, which make them unable to separate tiny water and oil droplet from water-in-oil and oil-in-water emulsions in one step.[2, 3] Separation technologies that rely on filtration-based systems can purify oil/water mixture in efficient, green, and low-cost energy processes.[4] Synthetic filters and membranes with outstanding wettability known as superhydrophilic-superoleophilic (SHP-SOP) are used extensively to separate oil–water mixtures and emulsions in various settings, including gasoline and fuel purification, and oil spill clean-up.[5] However, most materials and surfaces that have superhydrophobic properties in air can be easily deactivated or fouled with oil. Therefore, the process of overhauling and cleaning such membranes requires an enormous amount of time, money, and energy.[6] Additionally, as the density of water is higher than oil, the water molecules can form a barrier across horizontally-oriented SHP-SOP membranes, which can suppress oil permeation and decrease the flux of system.

Underwater separation of oil-in-water emulsions can now be accomplished with a green, potent, cost effective and reliable method. Recently, inspired by the advantages of the superoleophobic properties of fish scales and other aquatic creatures, researchers have produced biomimicry-based anti-oil-fouling surfaces[7, 8]. In fact, the existence of a micro/nanoscale

topographical framework on the surface of the fish scales provide high roughness and the ability to adsorb water molecules and making a thin layer of water on their surface, which suppresses the attachment and fouling of oils on the surface. Unfortunately, due to the higher surface tension of water than oils and the extremely low surface tension of the bioinspired oil-repellent surface and membrane, this type of material mostly prefers to repel water as well. Indeed, there have been a few studies on the preparation of sustainable superhydrophilic/underwater superoleophobic membrane with a water and oil contact angles less than 5° and greater than 150°, respectively.[2, 3, 9-15] Moreover, the preparation of surfaces featuring underoil superhydrophobic and underwater superoleophobic properties often have disadvantages including (i) complicated syntheses steps, (ii) expensive process, (iii) laborious procedures, (iv) the use of toxic and antagonistic chemical reagents, and (v) the necessity of complex facilities, all of which challenge the implementation of the hydrophobic/hydrophilic materials for oil/water separation.[16-21]

As an alternative, we report a smart SHP-SOP filter made from grape seeds that is simple to fabricate, green, low-cost, and mass-producible, demonstrating both underwater superoleophobic and underoil superhydrophobic properties. Grape seeds are a natural and sustainable biomass source and are considered a waste material by the wine and grape juice industries. In fact, the vineyards have to pay a grape pomace disposal fee; therefore, the precursor material for preparation of the NBF membrane has very low-price (~2-3 cent/kg) in large scale.[22-24] Additionally, grape seeds do not leach harmful compounds in water, making it a safe raw material for use in water treatment applications. We designed a simple and sustainable activation process that turns grape seeds into nanobiofibers (NBFs) without the use of carbonization or any toxic organic reagents or solvents. Instead, we simply treat ground dried grape seeds (*i.e.*, grape pomace, derived directly from winery-based biomass waste) with sodium hydroxide (NaOH) in a

one-pot reaction, from which we are able to easily obtain high purity NBFs as a value-added product. The individual NBFs show short fiber and uniform structure which can be stuck and packed on each other, making a porous and smart substrate (membrane). The produced membrane demonstrates a remarkable wettability property that can be easily switched from an underwater superoleophobic membrane to an underoil superhydrophobic filter. This happens as the continuous phase of emulsion changing from water to oil, introducing the membrane as a strong candidate for the purification of oil/water emulsions. Furthermore, this system features the unique capability to separate both oil-in-water and water-in-oil emulsions, without any pre- or post-treatment while still maintaining its high permeability and antifouling ability.

Additionally, we extend the application of this low-cost and green NBF powder to encapsulate water droplets and prepare marble liquid by a bio-originated superamphiphilic material in air for the first-time, instead of hydrophilic or hydrophobic materials[25-29], acting like a shell to stabilize high volume of water in a droplet (120 μL) under air. Furthermore, based on this unique property, we demonstrate the ability of the NBF material to serve as a soil additive to enhance moisture retention and study its ability to promote the growth of lentil seeds in otherwise dry conditions. Our findings indicate that in addition to the separation characteristics of the NBFs, they can also serve as a physical barrier in suppressing the evaporation of water to retain soil moisture. The fabrication of these NBFs is simple, inexpensive, scalable, and green, enabling the production of a novel multifunctional material.

2. Experimental section

2.1. Materials

The grape pomace was collected from the Cornell Wine Lab at Cornell University in Ithaca, New York. NaOH (98%), kerosene, vacuum pump oil, hexane, span 80, and all solvents were purchased

from Sigma-Aldrich. Corn oil was obtained from a local grocery store. All aqueous solutions were synthesized using distilled water.

2.2. Synthesis of NBFs

The grape seeds were separated by hand from the stems and skins of the grape pomace. Once the seeds were separated and rinsed with distilled water, they were dried overnight (~16 hours) at 77 °C. The dried biomaterial was then ground by mortar and pestle and sieved to a 20 mesh, or 841 μm, particle size. Then 20 grams of this separated grape seed was added to 300 mL of 0.1 M NaOH solution and stirred on a stir plate for 2 h at 100 °C to obtain the NBFs. The resulting NBFs were filtered and rinsed with water, ethanol, and acetone, and dried overnight at 77 °C. The final NBF material was stored at room temperature in a 50 mL plastic vial.

2.3. Preparation of NBF membrane

The NBFs (1 g) were poured onto a stainless-steel mesh No. 100 with diameter of 1 cm and make a fixed bed of the NBF by placing another stainless-steel mesh on the top to stabilize the NBF bed in position. The density (ρ_{layer}) and the porosity (ε_{layer}) of the NBF layer, the density of the NBFs powder (ρ_{NBF}), and the average pore radius (r_p) of the prepared NBF membrane were 0.615 g cm^{-3}, 91.8%, 0.67 g cm^{-3}, and 2.7 μm, respectively, based on the corresponding equations in Table S1. The average pore size (2.7 μm) was obtained by ImageJ software.

2.4. Characterization

The morphology and structure of the grape seed and the obtained NBFs were studied using a Zeiss Gemini 500 field emission scanning electron microscope (FE-SEM) equipped with energy dispersive X-ray spectroscopy (EDX), and transmission electron microscopy (TEM), FEI T12 Spirit TEM STEM, operated at 120 kV. X-ray photoelectron spectroscopy (XPS) was performed

using a Surface Science Instruments SSX-100 XPS system at an operating pressure of ~2× 10-9 Torr. The thermal behavior and stability were monitored by a thermogravimetric analysis (TGA Q500, TA Instruments, New Castle, DE, USA) and differential scanning calorimetry (DSC Q2000 TA Instruments, New Castle, DE, USA). The attenuated total reflectance-Fourier-transform infrared (ATR-FTIR) spectra were recorded between 400 to 4000 cm^{-1} with a resolution of 4 cm^{-1} using an IRAffinity-1S spectrometer equipped with a single-reflection ATR accessory (Shimadzu Corp., Kyoto, Japan). The contact angle was determined through a contact angle machine (model190CA, Rame- Hart Instrument, Netcong, NJ). The dynamic light scattering (DLS) of the emulsions were recorded at 25 °C by a zeta-sizer (Nano-ZS90, Malvern Instrument Ltd., United Kingdom) with a scattering angle of 90° and a He/Ne laser (λ = 633). The amount of water in the oil filtrated through the NBF membrane was calculated by a Karl Fischer Titrator. The pore size of the NBF membrane was obtained from the SEM images using ImageJ software. The 3D image of the NBF membrane was scanned by a Keyence VK-X260 Laser-Scanning confocal microscope (Keyence Corporation of America, USA). A UV-2600 spectrophotometer (Shimadzu, Japan) was used to monitor the concentration of oil and methylene blue in water. The oil separation efficiency and of the NBF was monitored by measuring the hexane concentration in emulsion and in filtrated water with the UV–vis absorption spectrometer (the red O was used to dye hexane).

2.5. Separation of Water-in-Oil Emulsions

To synthesize the surfactant stabilized water-in-oil emulsion, four various types of oils (hexane, kerosene, vacuum pump oil, and corn oil)) were mechanically mixed with 0.1 g of span 80 for 10 min, after which water was slowly added to the oil mixtures with continuous shaking to make a volume ratio of 1(water)/50(oil) ml/ml. Then the whole mixture was sonicated under a power of 450 W for 1h and vortexed for more than 3 h at 25 °C to generate a stable milky solution of water-

in-oil emulsion. The same procedure was used to prepare surfactant-free emulsions without the use of Span-80. The as-prepared emulsions were able to pass through the NBF membrane sandwiched between the two stainless steel meshes simply by gravity, with the transparent oils collected into a volumetric glass container. The height of the water-in-oil emulsion separation glass column was fixed at 73 cm (ΔP = 7.3 KPa) and the flux was monitored for each oil emulsion. The used NBF was regenerated by flushing it out with ethanol twice and drying at 80 °C in a vacuum oven for 3 h.

2.5. Separation of Oil-in-Water Emulsion

For the oil-in-water emulsion, 0.2 g span 80 was added into 100 mL water, and then 2 ml hexane was added to the mixture. The mixture was sonicated under a power of 450 W for 1 h and vortexed for more than 1 h at 25 °C to generate a stable milky solution of oil-in-water emulsion. The same procedure was used to prepare surfactant-free emulsions without the use of Span-80. The as-prepared emulsion was able to pass through the NBF membrane sandwiched between the two stainless steel meshes simply by gravity, with the transparent water collected into a volumetric glass container. The height of the water-in-oil emulsion separation glass column was fixed at 73 cm (ΔP = 7.3 KPa) and the flux was monitored. The used NBF was regenerated for twenty times by flushing it out with ethanol and water and drying at 80 °C in a vacuum oven for 3 h.

2.6. Preparation of liquid marble

The bed of NBF powder were prepared in a petri dish with 2-3 mm thickness and then sessile water droplets with various volumes, ranging from 5 to 120 μL, were gently rolled on the bed of NBF and within 10 seconds water droplet were completely encapsulated to generate liquid marbles.

2.7. Soil Growth studies and Plant Measurement

6 g of different treatments of soil (loam) and several lentil seeds (*Lens culinaris*), purchased from a local grocery store, were added to separate glass vessel (diameter of 1.5 cm and volume of 10 mL). The five soil treatments used were (T1) 100% soil (control), (T2) 60% NBF (top layer) and 40% soil (bottom layer), (T3) 50 % NBF (top layer) and 50% soil (bottom layer) and (T4) mixing the 50% NBF and 50% soil to study the effect of the added NBF on the growth of the lentil seeds. The lentil seeds were incubated for 20 days in the glass vessels illuminated with cool-white fluorescent light at a temperature of 27 ˚C. Initially 3 ml water was added to all the vessels. Through the incubation period, the glass vessels were manually watered 1 ml every 4 days to maintain moist conditions to grow the seeds. The lentil growth was measured at the end of the test period. Each treatment was repeated three times. Soil, Lentil seeds and plants were collected from each vessel after 20 days and the soil and NBF were gently removed by washing out with water so the height of the plant and roots were measured by a digital ruler (Neiko 01407A).

3. Results and discussion

To prepare the raw material for process, we ground the pre-separated grape seeds into a fine powder and sieved the material to a particle size less than 50 μm (Fig. 1, see Methods for details). We then removed impurities, pectin, lipid, lignin, contaminants, and pigments from the surface of the grape seed powder by stirring the raw material in NaOH solution, followed by filtration and drying to obtain the NBFs (Fig. 1A–D).[30-33] By comparing the ATR-FTIR of the grape seed with NBF significate differences were found at which the absorption bands at 783 cm^{-1} ($CH_{2\ rocking}$ of phenolics), 1317 cm^{-1} ($CH_{2\ scissoring}$ of polysaccharides, pectins), 1438 cm^{-1} (C-$C_{aromatic}$ of phenolics), 1605 cm^{-1} (COO^- and C=$C_{aromatic}$ of pectins and phenolics), 1742 cm^{-1} (C=O_{ester} of polyesters, pectins and lignins), 2852-2923cm^{-1} ($CH_{2\ aliphatic}$ of lignins and lipids) and 3003 cm^{-1} (=C-H of aromatic ring) were disappeared on NBF surface and chemically stable

backbone of the NBF remained (Fig. S1).[34-37] It is noteworthy to mention that NBF shows a very small and broad peak at 3300 cm^{-1} belonging to the –OH stretching vibration, compared to the commercial cellulose nanofibers and crude grape seed.[38] This peak shows that the NBF has a small amount of water content, leading to a lighter weight and more active carbon framework for further interactions. Moreover, disappearance of the peaks at 1743 and 1521 cm^{-1} which are attributed to the acetyl and uronic ester linkage of carboxylic group of the ferulic and p-coumeric acids of lignin, or to the hemicelluloses and aromatic rings of lignin respectively.[39] This confirms that active available material in the structure of NBF, more likely, is the cellulose structure.

We also studied the thermal stability of the grape seed and the NBF using TGA and DSC characterizations (Fig. S2). As shown in Fig. S2A, TGA and DTGA data revealed a moisture evaporation at low temperatures—from 25 to 100 °C—in which NBF has absorbed more moisture than the grape seed samples (potentially due to the removal of impurities like lipids from the NBF's oxygen framework).[30-32, 40, 41] Both the grape seed and NBF samples showed a rapid change at ~ 220–380 °C due to the degradation of their organic compounds. Grape seed sample shows three small steps, shown in DTGA data, as three small peaks at 408, 476 and 610 ºC that can be related to the oxidation and breakdown of charred residues.[40] The only observed degradation is caused by pyrolysis of the carbon framework of the NBF.[31] The slightly lower intensity in NBF DTGA peak (at 330 ºC) comparing to grape seed (346 ºC) is due to the faster heat transfer of the cellulose in NBF. Furthermore, NBF data also shows higher ash content because of the NaOH washing procedure and possible sodium interactions that has been further confirmed by SEM-EDX.[42]

The DSC curves (Fig. S2B) demonstrate a very low glass transition temperature (T_g) for both samples. NBF shows lower T_g (-36 °C) comparing to grape seed (-31 °C), probably due to the removal of impurities and lipids. The very low T_g shows that these cellulose-based materials can

be very effective for low temperature applications. The DSC curves of NBF show lower thermal stability compared to the grape seed due to changes in structure or degradation at 170 ˚C. Meanwhile, the grape seed is completely stable even at higher temperatures. There are two likely reasons for this behavior. First, higher surface area of NBF compared to the grape seed could increase the thermal conductivity and, therefore, the rate of heat transfer. The same property has been reported for cellulose nanocrystals.[43] Second, cellulose will decompose to levoglucosan around 180 ˚C which then gasifies efficiently at 300 ˚C. This may explain the sudden change in the weight appearing in the DSC curve of NBF. As there is no lipid or other protection, this change is more visible in NBF and this decomposition in grape seed might happen in higher temperatures.[42]

Compared to the pristine grape seed (Fig. S3), SEM and TEM images as well as SEM-EDX data of the treated grape seed showed pure nanofiber structures that were 0.5−3 μm long and 10−15 nm wide, which indicated that most of the impurities were remove from the surface of the grape seed, leaving pure NBFs remaining with high mechanical stability after long-term (one month) exposure in either acidic (pH = 2) or basic (pH = 13) solution under mechanical stirring condition (Fig. 1E-H and Fig. S4). Compared with the reported sizes for commercial cellulose nanofibers, NBF shows short, a unique, uniform, and unbranched individual nanofibers' structure, providing more advantages to NBFs.[38] Moreover, the removal of lipids, pectin, and other impurities are further confirmed by SEM-EDX (Table S2). The grape seed shows P, K, Si and Mg elements. NBF EDX results did not show any of these elements. The NBF membrane was obtained by sandwiching NBFs layer between two stainless steel mesh. A centimeter-sized NBF membrane was illustrated in Fig. 1I. The SEM image of the NBF membrane showed a microscale, porous framework resulting from the aggregation and stacking of NBF, Fig. 1J. Furthermore, laser scanning confocal microscopy was used to observe the NBF membrane's 3D topographical

framework, in which the average surface roughness of the NBF membrane of 12.2 μm, was observed (Fig. 1K).

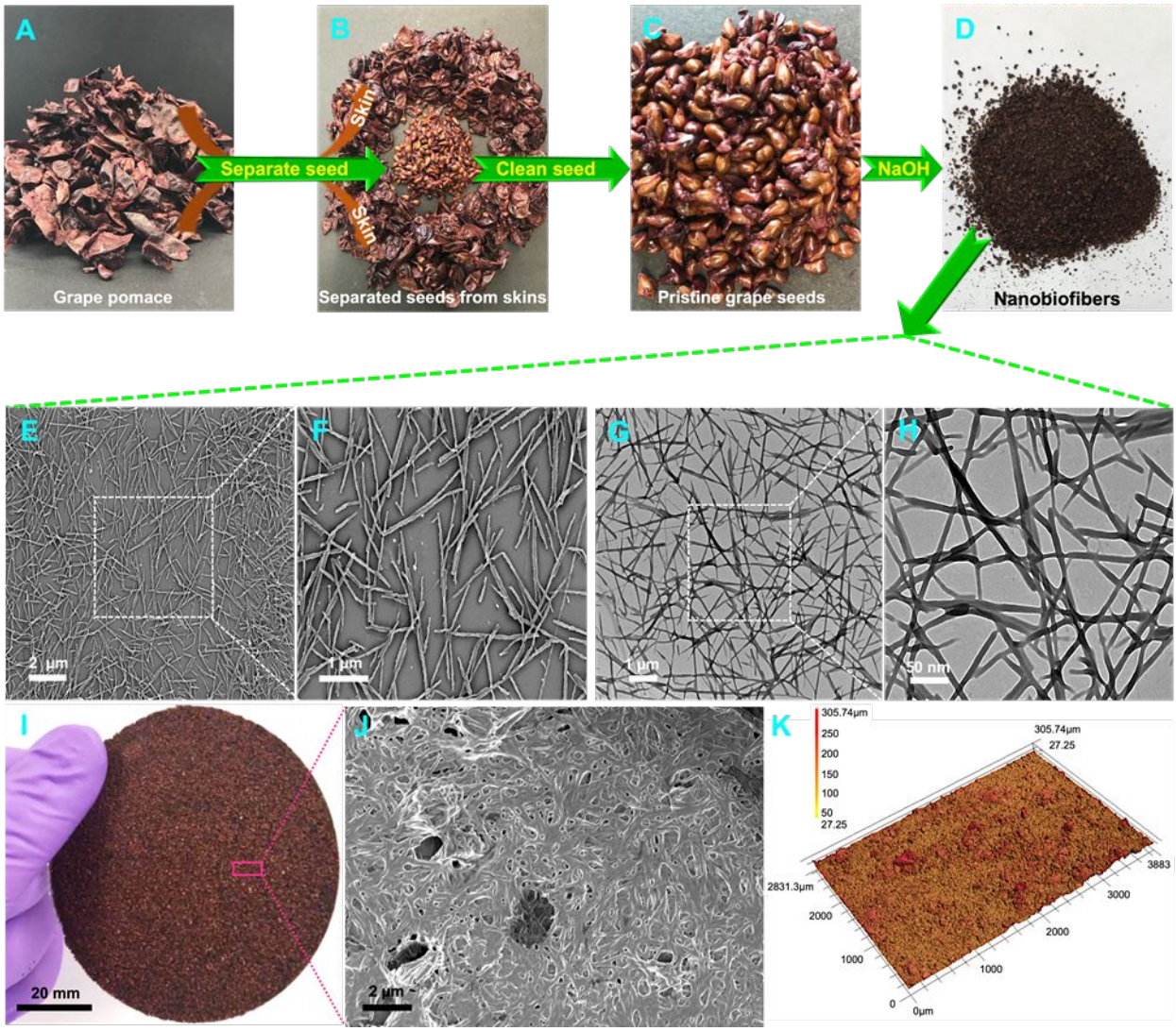

Fig. 1. (A–C) Schematic illustration of the preparation of NBFs from grape pomace. (D) Optical, (E, H) SEM, and (G, H) TEM images of the NBF powder, (I) photograph of a NBF membrane, (J) SEM of NBF membrane, and (K) 3D image of NBF membrane.

To assess the surface wettability of the NBF membrane, we measured the water and oil contact angle in air (Fig. 2A–B). Both water and oil droplets (2 μL) penetrate and diffuse within

130 ms on the surface of the NBF membrane, resulting in a contact angle of nearly 0° in both cases (Movies S1 and S2). When water is dropped on the NBF membrane, the membrane's surface adsorbs the water and starts to swell within a millisecond (Fig. 2A). Indeed, the NBF membrane is superamphiphilic in air because of its large surface energy from the high concentration of hydroxyl groups on the surface of the NBFs.[44] Furthermore, the superhydrophilic NBF membrane shows unique underwater superoleophobicity, with an oil contact angle as high as 153° or higher when different types of oil, (*e.g.*, kerosene, corn oil, pump oil, hexane, and petroleum ether) were used (Fig. 2C). This behavior suggested the membrane's potential in oil/water emulsion separation underwater.[45] Due to the material's high surface energy, the high content of water molecules trapped on the surface of the NBF and the rough micro/nanostructures of the NBFs reduce the contact area of the oil droplet with the surface of the membrane make a unique superoleophobic surface with a large oil contact angle under water.[9, 46-48] However, we also found the water contact angle of the NBF membrane under oil was 165°, which demonstrates the superhydrophobicity of the NBF membrane (Fig. 2D, Movie S3). In this case under oil, the trapped layer of oil molecules on the surface of the membrane appear to act as a repulsive liquid phase that suppresses the penetration of water through the membrane surface, resulting in under oil superhydrophobicity.

To evaluate the surface wettability of the NBF membrane in detail, we also studied the wetting behavior and dynamic interaction of the oil-in-water emulsion and water-in-oil emulsion droplets on the membrane. When a droplet of oil-in-water emulsion contacts the surface of the membrane, water molecules penetrate through the nanostructure of the membrane within 31 ms and the wetted membrane starts to swell within 66 ms and consequently the oil particles retain and aggregate on the surface of the membrane (Fig. 2E, Movie 4). The reverse situation occurs in the case of dropping a water-in-oil emulsion on the surface of the membrane in which the oil

immediately passes through the membrane within 33 ms and the water droplets are blocked on the surface of the membrane (Fig. 2F, Movie S5). As a result, we conclude that whatever the continuous or dispersed phase (oil or water) the membrane is able to separate various emulsions. When the continuous phase is water in an oil-in-water emulsion, the NBF membrane will be superhydrophilic and under-water superoleophobic, enabling the filtration of the oil from the water phase. However, in a water-in-oil emulsion the continuous oil phase changes the respond of the NBF membrane to be superoleophilic and underoil superhydrophobic, accelerating the penetration of oil and the separation of water.

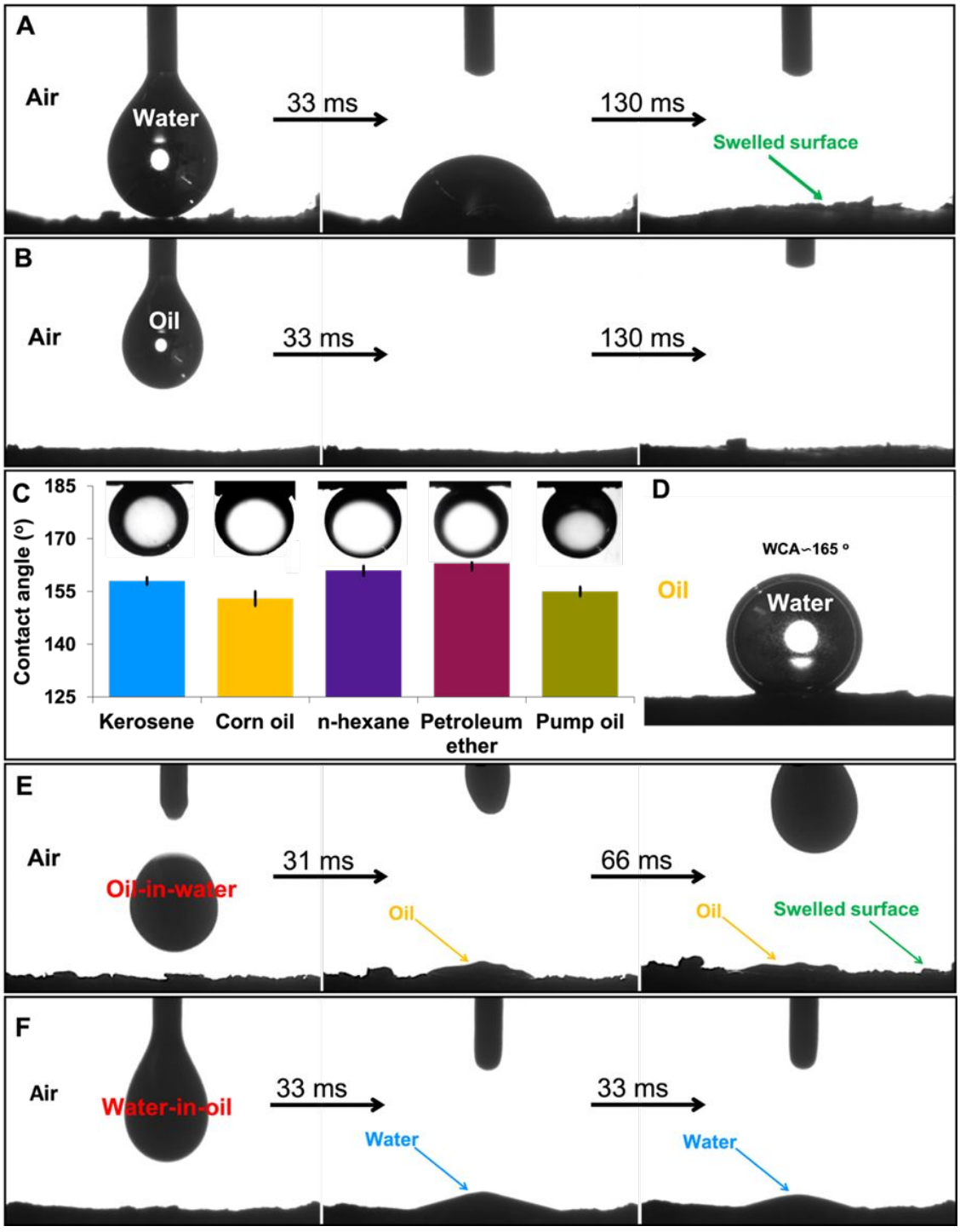

Fig. 2. (A–B) Photographs of the dynamic measurements of water and oil permeation on the surface of the NBF membrane. (C) Variation of the different underwater oil contact angles. (D)

The water contact angle underoil of the NBF membrane. (E) The oil-in-water and (F) water-in-oil permeation on the surface of NBF membrane.

These results show how we are able to successfully prepare a green, low-cost, smart, and switchable membrane at room temperature from biomass (grape pomace) using a simple process without the use of any toxic or chemically hazardous reagents. As a result, we anticipate our unique synthesis could be used to fabricate membranes in developing countries for the separation of oil/water and water/oil emulsions.

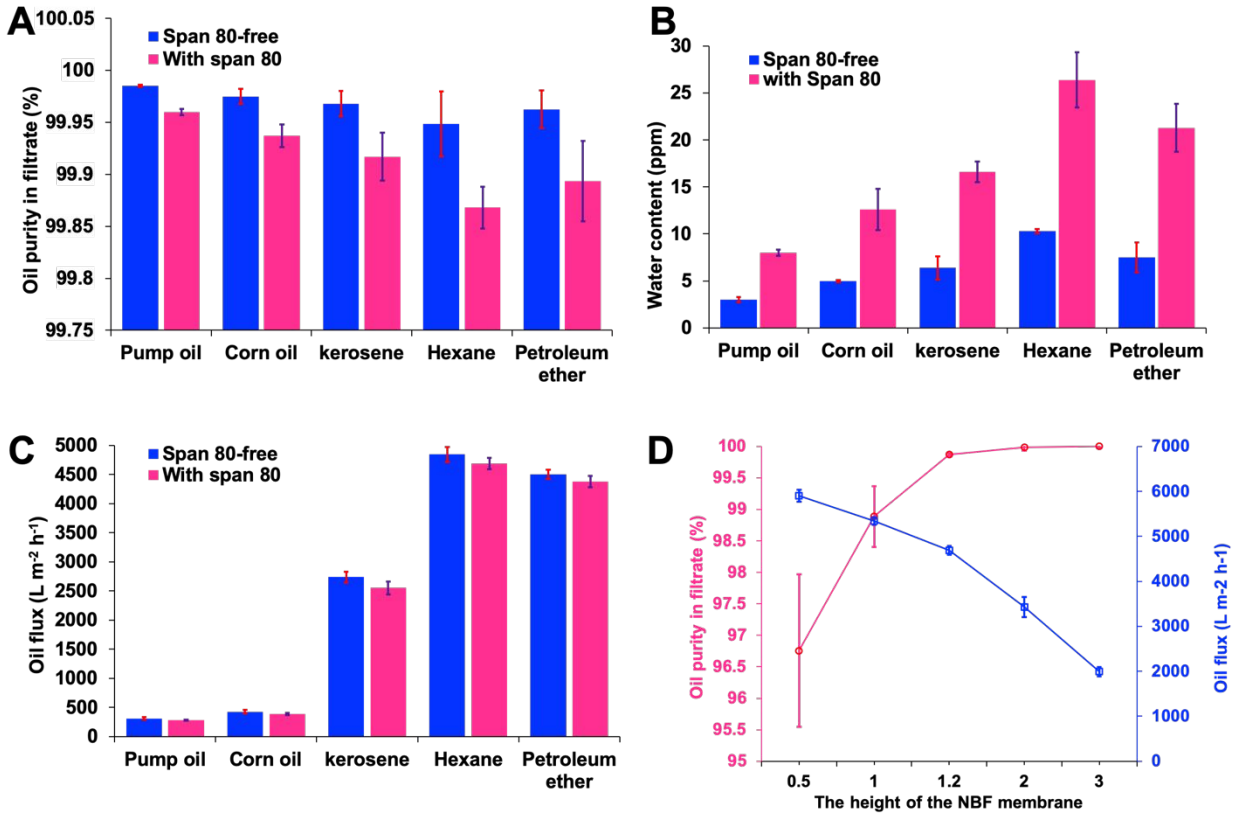

Fig. 3. (A) Separation capabilities of the NBF membrane for span 80-stabilized and span 80-free water/oil emulsions made with different oils. (B) Water content in the filtrates of span 80-stabilized and span 80-free water/oil emulsions. (C) Oil permeation flux of the NBF membrane for span 80-stabilized and span 80-free water/oil emulsions. (D) The effect of the height of the NBF membrane on its separation capability and oil flux for span 80-stabilized water/hexane emulsions.

We also studied the functionality of our NBF membrane for the separation of different types of oil from surfactant-free water/oil mixtures and surfactant-stabilized water-in-oil emulsions. To investigate the filtration performance of the NBF membrane, pump oil, corn oil, kerosene, hexane, and petroleum ether were selected to make an emulsion with or without stabilization using Span 80 as the surfactant. Fig. 3A shows the oil purity in the filtrate after passing different stabilized and non-stabilized water-in-oil through NBF membrane. The NBF membrane showed significant oil purification performance (99.9%) for all types of oil with or without the use of surfactant. We also found that for Span 80-free samples, the oil purity in the filtrate stayed between 99.95% to 100% for all types of oils. On the other hand, for surfactant-stabilized materials, the oil purity slightly decreased, with the NBF membrane displaying the highest and lowest purity for pump oil (99.96%) and hexane (99.87%), respectively.

Fig. 3B shows the water content in the filtrate after passing different stabilized/non-stabilized oils through the NBF membrane. The water content is less than 10 ppm for the surfactant-free samples, which confirms the results described above. Meanwhile, the lowest water contents of 3 and 5 ppm were achieved when vacuum pump oil and corn oil were used, respectively. Likewise, similar to the phenomenon observed before, the water content in the filtrate for the water-in-hexane emulsion with span 80 was the highest (10.3 ppm). As a result, we found that with the use of the surfactant Span 80, the water content for the pump oil emulsion increased from 3 to 8 ppm while for hexane it went up from 10 to 26.4 ppm. We also investigated the permeability of the NBF membrane to evaluate the filtrate flux of the water-in-oil emulsion separation process (Table S1 and Fig. 3C). Our results indicated that the permeate flux of the membrane did not depend significantly on whether or not surfactant was used in the different

water-in-oil emulsions explored. However, the flux is heavily dependent on the oil's viscosity. Consequently, the fluxes for the pump oil and corn oil (312 ± 21 and 428 ± 30 L m^{-2} h^{-1}, respectively) were essentially far lower than that of the less viscous hexane and petroleum ether emulsions, which demonstrated flux values of 4844 ± 127 and 4501 ± 87.5 L m^{-2} h^{-1}, respectively (Fig. 3C). We also note that compared to the permeation properties of previously reported superhydrophilic membranes [3, 18, 49], the flux results shown here demonstrate the extraordinary permeability of the NBF membrane without the use of any external pressure.

We believe that the difference in oil purity among the various used water-in-oil emulsions directly depends on their viscosity. As hexane has the lowest viscosity amongst these oils, the flux through the membrane is higher and the passing emulsion has less time to interact with NBFs. On the other hand, pump oil and corn oil possess higher viscosities and thus have enough time to interact with the membrane, which results in higher filtration performance for these oils. Moreover, the use of surfactant helps stabilize the smaller water droplets, which makes it harder to filter them from the passing fluid. Therefore, a slight drop in oil purity was seen when using surfactant-stabilized emulsions. However, we note that the oil purity in the filtrate was well over 99.85% for all samples, which is promising for the use of our very low-cost and sustainable membrane, in comparison to the other reported systems [2, 49, 50], at large scale specially in resource-limited countries/settings.

In order to investigate the effect of the height of the NBF membrane on its separation capability and oil flux, we representatively chose the Span 80-stabilized water/hexane emulsion sample. As shown in Fig. 2D, we increased the bed height of the NBF membrane from 0.5 to 1.2 cm, the oil purity in the filtrate increased from 96.75% to 99.87%. Furthermore, when we increased the bed height further above 1.2 cm, the oil purity of the filtrate reached 100%. This can be

attributed to the longer contact time and greater interaction of the emulsion feed with the thicker NBF membrane. On the other hand, after increasing the bed height from 0.5 to 1.2 cm, the oil flux slightly decreased from 5901 to 4687 L m^{-2} h^{-1}, and by further increasing the height to 3 cm, the oil flux drastically decreased to 1993 L m^{-2} h^{-1}. This phenomenon is reasonable since increasing the membrane bed height leads to a higher pressure drop, in which the friction forces reduce the flux of a liquid through a column, and consequently the flux drops significantly.[51] We further studied the relation between the emulsion feed flux and the height of the NBF membrane using the Hagen–Poiseuille equation (Table S1), which based on the equation and our results on using different oils (Fig. 3C, Movie S6) and NBF heights (Fig. 3D), we found the flux displays an inverse proportional correlation with the viscosity of oil and the height of the NBF bed. Therefore, the flux is only affected by the oil viscosity and thickness of the membrane.[52]

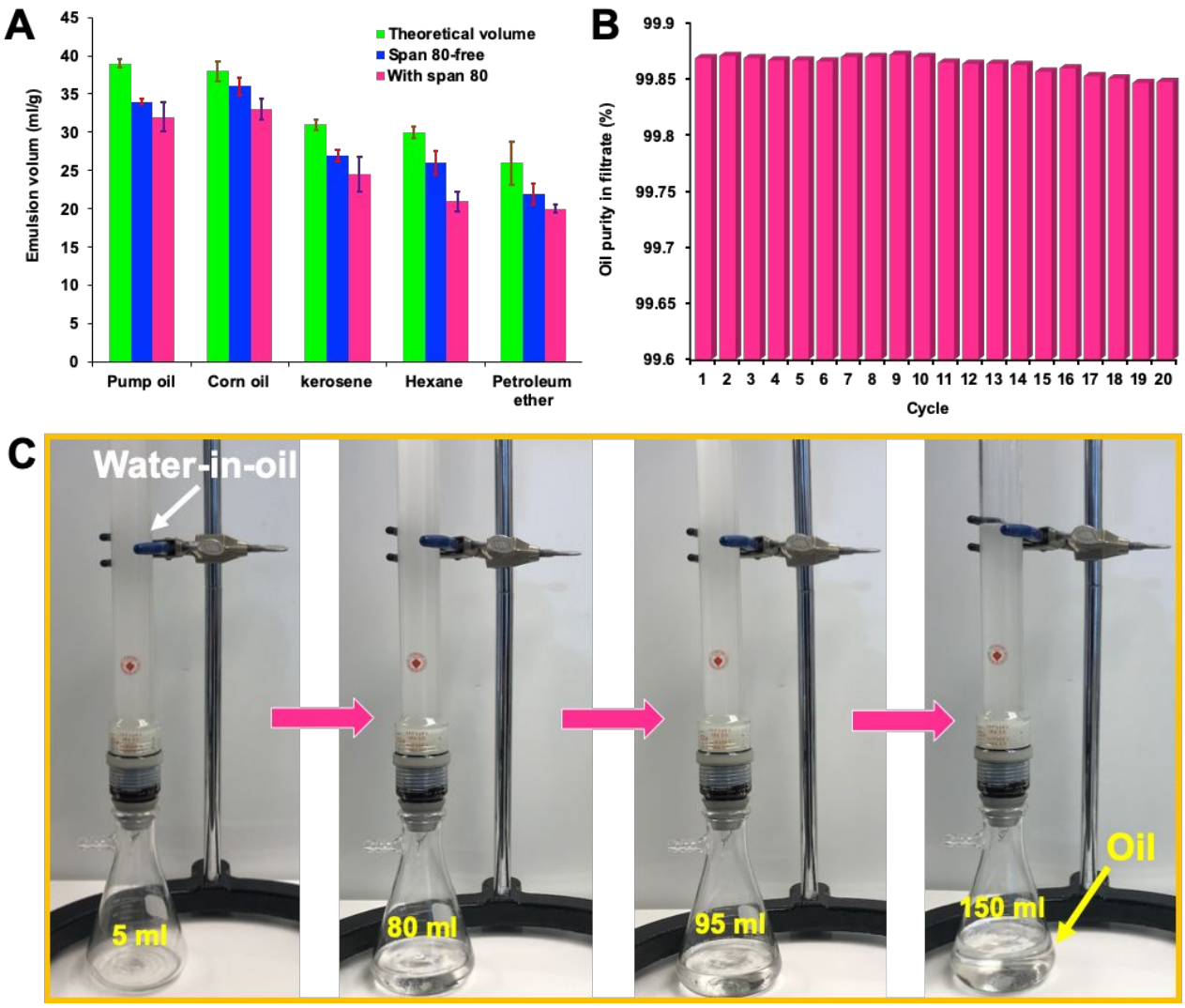

Fig. 4. (A). The theoretical and experimental amount of filtrated oil volumes by the NBF membrane for span 80-stabilized and span 80-free water/oil emulsions. (B) The change in oil purity of the Span 80-stabilized water/hexane emulsion filtrate over twenty filtration cycles using the same NBF membrane. (C) Photos illustrating the process of separating the Span 80-stabilized hexane-in-water emulsion using the NBF membrane (height of 1.2 cm).

Due to the fact that every membrane has a saturation point and is only capable of adsorbing a certain amount of water, we calculated the theoretical value of the separation capacities of various water-in-oil emulsions by NBF membrane (see Table S1). To achieve the

experimentally NBF membrane water adsorption saturation point (m_0) in the emulsion separation process, we considered the first drop of filtrate which turned from transparent to turbid (or milky color of the pristine emulsion) as an indication of the end of separation and thus the membrane's saturation point. Fig. 4A shows the theoretical and experimental amounts of filtrated volumes before saturation of NBF membrane for different water-in-oil emulsions both with and without Span 80. The NBF membrane exhibited lower separation capacities for the Span 80-stabilized samples (20–32 mL (oil)/g (NBF membrane)) compared to the Span 80-free (22–36 mL/g) water-in-oil emulsions. As described earlier, the separation performance of the Span 80-stabilized water-in-oil emulsions was generally lower than that of the span 80-free emulsions because the surfactant leads to smaller stabilized water droplets.[53] Thus, these stable microdroplets of water dispersed in the Span 80-stabilized emulsions do not have enough time to merge and aggregate to form larger droplets compared to the Span 80-free samples at NBF membrane interface.

To be economically viable, separation membranes must be reused multiple times, ideally without significant degradation in performance. To explore the recyclability of our NBF membrane for the separation of water-in-oil emulsions, we used the Span 80-stabilized water-in-hexane sample as a model feed liquid and measured the oil filtrate purity after twenty cycles of filtration (Fig. 4B). After each cycle, the NBF membrane was washed by ethanol and then dried at 75 °C to prepare the filter for the next use. Fig. 4B shows that over twenty cycles, the NBF membrane maintained significantly stable performance, with an oil purity that ranged between 99.85% and 99.87% in the filtrate liquid.

Furthermore, as illustrated in Fig. 4C, the NBF membrane shows potent mechanical stability and separation efficiency in the separation of water from oil when a long glass tube with

height of 73 cm was installed and the water-in-oil emulsion was poured directly into this homemade system. Based on the intruding pressure equation (Table S1), we estimate that the durability of the NBF membrane could be last and preserve its ability under the high intruding pressure of 7.32 kPa, which is higher than most previously reported superhydrophilic membrane [3, 54, 55], suggesting the proposed material should demonstrate excellent performance at large scale.

We also monitored the water-in-oil emulsions before and after filtration process using optical microscopy and DLS (Fig. S5). The water droplet sizes of the hexane and pump oil solutions were smaller than 6 nm, while for corn, petroleum ether, and kerosene the droplet size was significantly greater at ~1000 nm, which could be due to the difficulty of achieving water droplet dispersions in these oils at the conditions used. Interestingly, no water droplet were dispersed in the filtrated solution after passing the feed emulsion through the NBF membrane because the zeta sizer instrument did not give us any particle size which again confirmed the unique and remarkable ability of the membrane in purification of the oil.

To better characterize the switchability of the NBF membrane from superhydrophilicity to superhydrphobicity, we studied the separation of the hexane-in-water emulsion stabilized with Span 80. By pouring the oil-in-water emulsion feed onto the NBF membrane immediately transparent water passed through the membrane while oil was blocked on the membrane's surface, which the performance of the NBF membrane we further confirmed by comparing digital and microscopic images of the dense oil droplets in the emulsion feed, which appeared milky-white, with the transparent solution of the filtrated water, which featured no droplets (Fig. 5A, Movie S7). Furthermore, DLS data revealed that only a few 1 nm oil droplets were observed in the purified water after ultrafast filtration process by the NBF membrane (Fig. 5B).

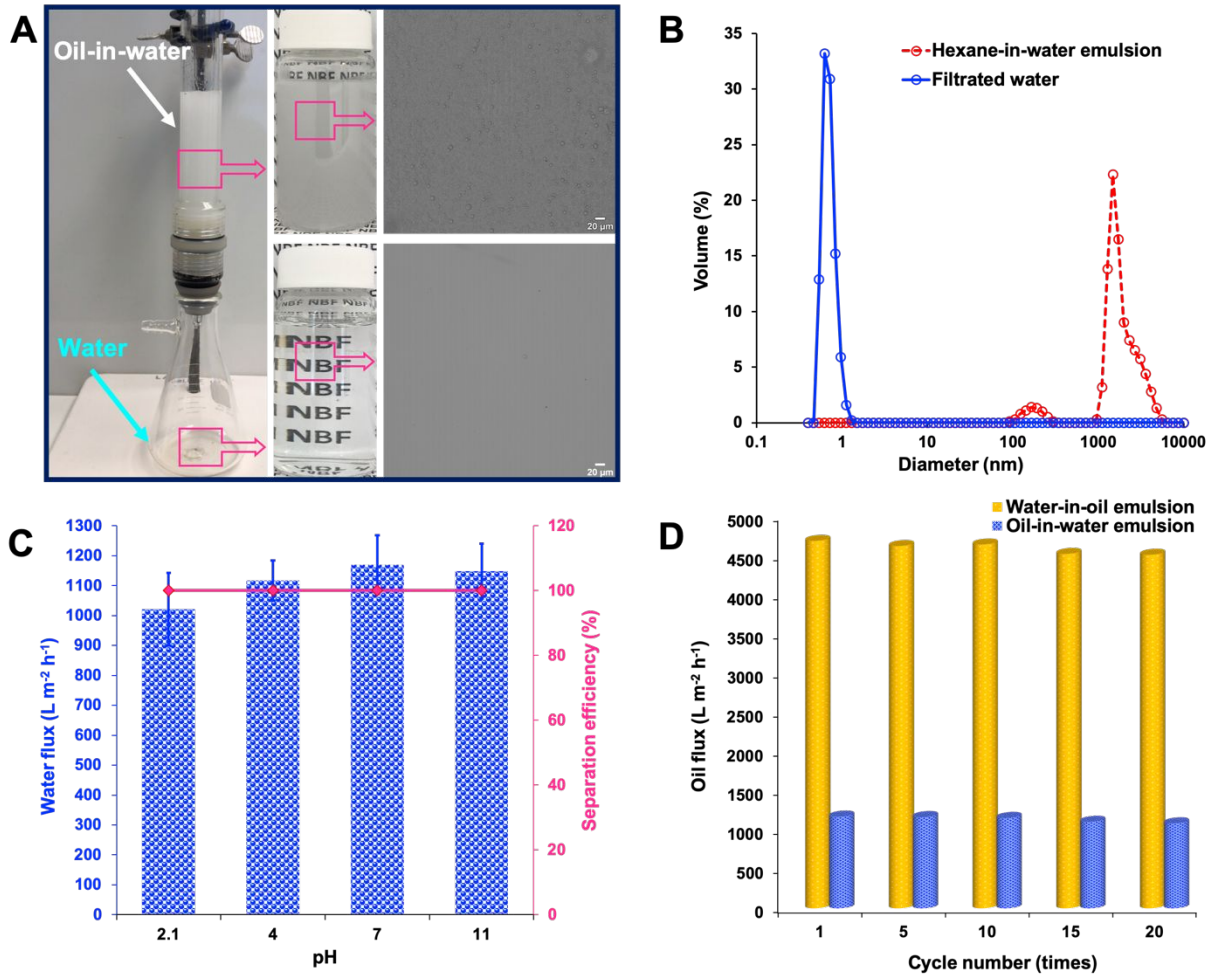

Fig. 5. (A) The purification process by a lab-made filtration unit and microscopy images of a stabilized hexane-in-water emulsion stabilized with Span 80 before (top) and after (bottom) separation. (B) Particle size analysis of the Span 80-stabilized hexane-in-water emulsion feed and filtrated water. (C) The permeation flux and separation efficiency of the NBF membrane for Span 80-stabilized hexane-in-water emulsion at different pH values. (D) The permeation flux of the NBF membrane for the Span 80-stabilized water-in-hexane and hexane-in-water emulsions after multiple cycles of filtration.

We also evaluated the chemical stability of the NBF membrane at different pH using a hexane-in-water emulsion made with water that ranged in pH from 2.1 to 11.0 (Fig. 5C). The water

permeation flux slightly increased from 1021 L m^{-2} h^{-1} to 1150 L m^{-2} h^{-1} as the pH values increased from 2.1 to 11.0. Additionally, we found that the membrane demonstrated stable oil separation performance, with 100% water filtrate purity for all pH values ranging from 2.1–11.0, suggesting the excellent chemical stability of the membrane under basic and acidic conditions, allowing it to retain its ability to filtrate water with high purity.

To further evaluate the practical application of the proposed membrane we measured the permeate flux for both the water-in-hexane and hexane-in-water emulsions after 20 cycles of separation process. (Fig. 5D). In addition to high water-in-oil and oil-in-water emulsion purification performance of the membrane, we found the permeability for both emulsions was noticeably unchanged as we increased the number of filtration cycles. This finding suggests the NBF membrane has excellent antifouling properties, to which the low oil-adhesion and water-adhesion under opposite phase characteristics of the NBF membrane substantially contribute to its performance. The high purity of the filtrates and the high permeate flux verify the membrane's capability to filter both water-in-oil and oil-in-water emulsions, facilely switching its transport properties upon exposure to these various solutions.

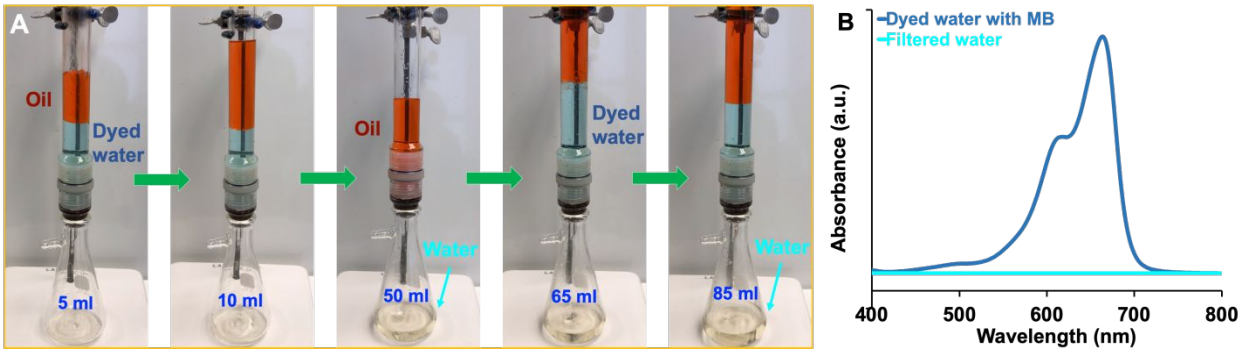

Fig. 6. (A) Photographs demonstrating the simultaneous oil/dye/water separation process using the NBF membrane (for clarity, the hexane oil phase was dyed red and the water phase contained the MB dye). (B) The UV–vis spectra of the MB dyed water before and after the filtration process.

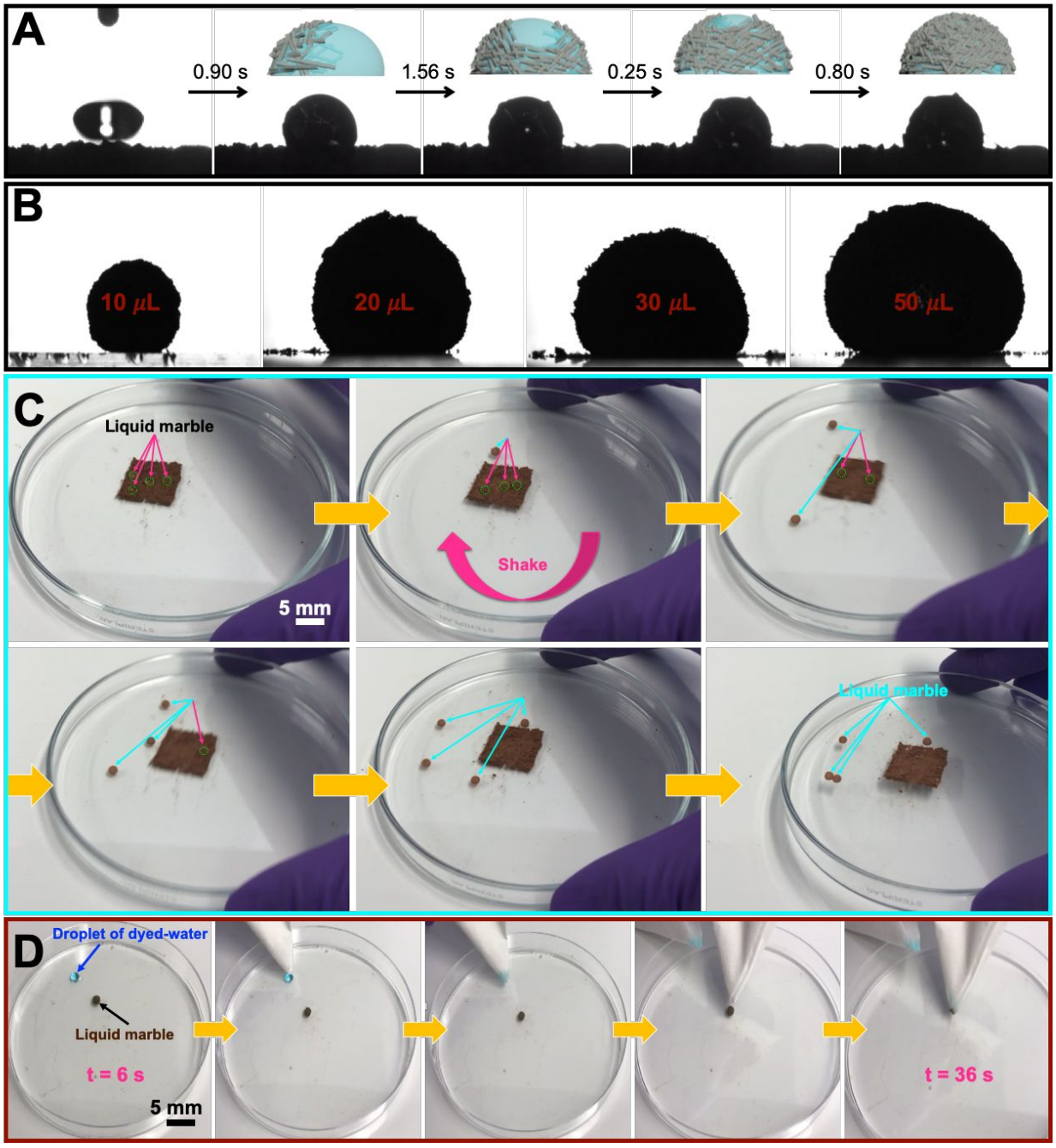

Fig. 7. (A) Image sequence of liquid marble preparation by spontaneously migration of NBF to the water-air interface, and then encapsulates the water, (B) NBF-based liquid marbles prepared by encapsulation of water volumes ranging from 10 to 50 μL, (C) preparation of a liquid marble by rolling a water droplet on NBF powder which then became perfectly non-wetting while

transferred on a glass petri dish, and (D) Snapshots indicating the color altering of aqueous methylene blue droplet without and in a NBF-based marble liquid after 36 seconds.

In addition to its excellent and versatile filtration properties, the NBF membrane also displays efficient adsorption towards methylene blue (MB)—a toxic and carcinogenic positively charged dye commonly use in the textile industry. Due to the negative surface charge of the NBFs (ζ-potential of NBF is -37 mV at pH 7.0), the membrane is able to simultaneously separate oil and dye from water in ultra-second(Fig. 6A, Movie S8).[15] By several times refeeding the membrane with oil/dyed-water the oil and dye (4 ppm) will be rejected and adsorbed by NBF, respectively, and colorless water is obtained. The obtained adsorption capacity of the NBFs towards MB was 67 mg/g. Additionally, Fig. 6B shows the UV–visible spectra of the feed and filtrated water solutions, in which the mother solution of MB (4 ppm) shows an adsorption peak at 665 nm while this peak in the filtrated water is completely omitted, proving the successful separation of the dye from the oil/water mixture.

We found out that by dropping water droplet (2 μL) on the powder bed of the NBF under air the water droplet is coated and stabilized with NBF particles after 3-4 second and make an encapsulated water droplet that did not diffuse through the NBF powder (Fig. 7A, Movie S9).[26-28] When we make a pellet bed from the NBF powder such behavior will not occur and water droplet penetrate through the NBF bed within millisecond (Fig. 7A). In fact, the powder bed surface was wetted immediately by penetrating of the water droplet and due to the capillary and viscous forces the wetted NBF particles start to move up around the water droplet, in which agitation of NBF powder accelerates the process of particle aggregation into clusters (schematic of inserted in Fig. 7A). The water molecules bind the NBF together as a bridge while water

molecules cannot diffuse and approach into poorly wetting NBF, therefore water droplet was encapsulated by the shells of NBF as a liquid marble and stabilized without leaking fluid.[56] To the best of our knowledge, it is the first report of preparing a marble droplet with a bio-originated, superamphiphilic material (*i.e.*, previous reported liquid marble were prepared with either hydrophilic or hydrophobic materials). [25, 29]

Furthermore, by dropping various volume of water droplets from 10 to 80 μL on the powder bed of the NBF spherical water droplet are prepared where the contact angle of all the marble droplets were above 160º (Fig. 7B). While on marble droplets with volume larger than 10 μL showed slight distortions from spherical shape due to the gravity and flexible puddle-like structure of the prepared marble droplet.[57] This implies the combination of superamphiphilic, uniform, unbranched, and light weight properties of the NBF, in air, are essential for generation of liquid marble. Therefore, we studied this unique property of the NBF more in details. As the typical digital photographs and schematically illustrated in Fig. 7C, the liquid marbles were created simply by pouring a droplet of water or rolling water droplets on a bed powder of NBF and the NBF spontaneously self-oriented by the capillary forces and act like shell which eventually more NBF are attached on the surface of the water marble to prepare NBF multilayers and stabilized the water droplet at the water/air interface to encapsulate the core of water droplet and suppressed the water droplet from wetting its environment owing to their super hydrophilicity under air.[58, 59] Fig. 7C illustrates a digital photograph of four liquid marbles with a diameter of about 2.5 mm prepared, which could be rolled out freely by simply shaking on the surface of a glass dish (Movie S10). The weight ratio of the NBF shell and the core of the inner water droplet was about 1:10.

Another remarkable application of NBF is the ability of NBF-based liquid marbles as adsorbent miniature reactors towards the adsorption of encapsulated and trapped aqueous MB 7

mL of dyed-liquid marbles containing 5 ppm MB solution are synthesized (Fig. 7D, Movie S11).[57] Then the dyed-liquid marbles are ruptured at pre-determined reaction time and the encapsulated MB solutions are gathered, where the color intensity of the MB solution after 36 second is visibly decreased and turns colorless after 45 second, resulted that more than 99% of the MB was removed. Indeed, our proposed system benefits from the superior adsorption ability of NBF, large surface area-to-volume ratios of NBF, and its property to generate a low-cost, biooriginated and mechanically stable liquid marble shells to have the proper and potent interaction with contamination of water droplet. However, the obtained result indicated that NBF could encapsulate 123 μL of water when the particle size of the NBF is around 50 μm (Fig. S6, Movie S12). Indeed, larger particle size showed higher adsorption energy and packing density onto the surface of water droplet, therefore it would need larger force to detach and disorder particles of NBF, which meanwhile acts as a physical barrier to water evaporation from water surface to rupture the obtained large marble liquid.[59]

Water stress is a critical problem for plant growth in dry and arid weather and soils.[60] Therefore, based on the property of the NBF in encapsulation of high volume of water droplet we set up an experiment to demonstrate a concept that NBF is being able to retain the humidity and water of the soil in dry situation and release it slowly based on the need of the used plant when they add on the surface of soil or mixing with in comparison with the pristine soil (see the Supporting Information).[61] For treatments of T1 and T2 after 20 days there are no sign of growing lentil while in treatments T3 and T4 the growth of lentil was profuse when NBF were added to the same amount of soil or mixing with soil (Fig. S7). By measuring the height of lentil plant for treatments of T3 (57 mm) and T4 (73 mm) and comparison with treatment T1 (1.6 mm) the lentil in T3 and T4 growth 37 and 49 times more, respectively. The height of root for T3 and T4 reached

to 12 mm and 21 mm, respectively, which are 11 and 20 times more growth compared to when only soil is used as the treatment. It is very evident that the presence of NBF when mixing with soil significantly increased the growth of lentil in arid situation by retaining the humidity and water which acts as a physical barrier to water evaporation around the lentil seeds and keep them alive.[56]

Acknowledgments

We thank the Cornell Center for Materials Research (CCMR) for use of their facilities. CCMR facilities are supported by the National Science Foundation under award number DMR-1719875.

Conclusion

We present a low-cost, green NBF membrane made from biomass using a simple, one-pot reaction without the use of any toxic reagent or solvent, or any specialized equipment. The resulting material demonstrated excellent separation capability of different, stabilized, oily wastewater emulsions, as well as being able to simultaneously and rapidly separate dye from the oil/water mixture by gravity. Additionally, for the first time we prepared a liquid marble as a miniature reactor using a bio-originated superamphiphilic material instead of commonly used hydrophilic or superhydrophobic material to remove dye from wastewater. As an added functionality, we demonstrated the ability of the NBF material to encapsulate a high volume of water droplet (120 μL), allowing it to be used a soil additive for enhanced water retention, enabling us to grow a lentil plant in arid conditions. This work provides a low-cost sustainable material for the smart separation of stabilized emulsions in addition to its other multifunctional uses, suggesting its great potential for future applications in other fields.

References

[1] D.S. Sholl, R.P. Lively, Nature, 532 (2016) 435–437
[2] M. Tao, L. Xue, F. Liu, L. Jiang, Advanced Materials, 26 (2014) 2943-2948.
[3] W. Zhang, N. Liu, Y. Cao, Y. Chen, L. Xu, X. Lin, L. Feng, Advanced Materials, 27 (2015) 7349-7355.
[4] J.R. Werber, C.O. Osuji, M. Elimelech, Nature Reviews Materials, 1 (2016) 16018.
[5] Z. Zhu, S. Zheng, S. Peng, Y. Zhao, Y. Tian, Advanced Materials, 29 (2017) 1703120.
[6] Z. Chu, Y. Feng, S. Seeger, Angewandte Chemie International Edition, 54 (2015) 2328-2338.
[7] X. Yao, Y. Song, L. Jiang, Advanced Materials, 23 (2011) 719-734.
[8] L. Wen, Y. Tian, L. Jiang, Angewandte Chemie International Edition, 54 (2015) 3387-3399.
[9] F. Li, Z. Wang, S. Huang, Y. Pan, X. Zhao, Advanced Functional Materials, 28 (2018) 1706867.
[10] F. Zhang, W.B. Zhang, Z. Shi, D. Wang, J. Jin, L. Jiang, Advanced Materials, 25 (2013) 4192-4198.
[11] M. Liu, Y. Hou, J. Li, Z. Guo, Langmuir, 33 (2017) 3702-3710.
[12] P. Zhou, J. Li, W. Yang, L. Zhu, H. Tang, Langmuir, 34 (2018) 2841-2848.
[13] Y. Dong, C. Huang, X.-Y. Yang, Chemical Engineering Journal, 361 (2019) 322-328.
[14] Y. Long, Y. Shen, H. Tian, Y. Yang, H. Feng, J. Li, Journal of Membrane Science, 565 (2018) 85-94.
[15] X. Wang, M. Li, Y. Shen, Y. Yang, H. Feng, J. Li, Green Chemistry, 21 (2019) 3190-3199.
[16] P. Zhang, S. Wang, S. Wang, L. Jiang, Small, 11 (2015) 1939-1946.
[17] W. Zhang, N. Liu, Q. Zhang, R. Qu, Y. Liu, X. Li, Y. Wei, L. Feng, L. Jiang, Angewandte Chemie International Edition, 57 (2018) 5740-5745.
[18] G. Kwon, A.K. Kota, Y. Li, A. Sohani, J.M. Mabry, A. Tuteja, Advanced Materials, 24 (2012) 3666-3671.
[19] Z. Lei, G. Zhang, Y. Deng, C. Wang, ACS Applied Materials & Interfaces, 9 (2017) 8967-8974.
[20] H. Kang, Y. Liu, H. Lai, X. Yu, Z. Cheng, L. Jiang, ACS Nano, 12 (2018) 1074-1082.
[21] G. Cao, Y. Wang, C. Wang, S.-H. Ho, Journal of Materials Chemistry A, 7 (2019) 11305-11313.
[22] C. Beres, G.N.S. Costa, I. Cabezudo, N.K. da Silva-James, A.S.C. Teles, A.P.G. Cruz, C. Mellinger-Silva, R.V. Tonon, L.M.C. Cabral, S.P. Freitas, Waste Management, 68 (2017) 581-594.
[23] R. Devesa-Rey, X. Vecino, J.L. Varela-Alende, M.T. Barral, J.M. Cruz, A.B. Moldes, Waste Management, 31 (2011) 2327-2335.
[24] G.A. Martinez, S. Rebecchi, D. Decorti, J.M.B. Domingos, A. Natolino, D. Del Rio, L. Bertin, C. Da Porto, F. Fava, Green Chemistry, 18 (2016) 261-270.
[25] E. Bormashenko, R. Pogreb, A. Musin, R. Balter, G. Whyman, D. Aurbach, Powder Technology, 203 (2010) 529-533.
[26] Z. Liu, T. Yang, Y. Huang, Y. Liu, L. Chen, L. Deng, H.C. Shum, T. Kong, Advanced Functional Materials, 29 (2019) 1901101.
[27] Y. Wang, K. Ma, J.H. Xin, Advanced Functional Materials, 28 (2018) 1705128.
[28] X. Rong, R. Ettelaie, S.V. Lishchuk, H. Cheng, N. Zhao, F. Xiao, F. Cheng, H. Yang, Nature Communications, 10 (2019) 1854.
[29] P. Aussillous, D. Quéré, Nature, 411 (2001) 924-927.

[30] M. Soleymanzadeh, M. Arshadi, J.W.L. Salvacion, F. SalimiVahid, Chemical Engineering Research and Design, 93 (2015) 696-709.
[31] H. Eskandarloo, M. Arshadi, M. Azizi, M. Enayati, A. Abbaspourrad, ACS Sustainable Chemistry & Engineering, 7 (2019) 3895-3908.
[32] M. Arshadi, J.E. Gholtash, H. Zandi, S. Foroughifard, RSC Advances, 5 (2015) 43290-43302.
[33] M. Arshadi, S. Foroughifard, J. Etemad Gholtash, A. Abbaspourrad, Journal of Colloid and Interface Science, 452 (2015) 69-77.
[34] C. Tan, M. Arshadi, M.C. Lee, M. Godec, M. Azizi, B. Yan, H. Eskandarloo, T.W. Deisenroth, R.H. Darji, T.V. Pho, A. Abbaspourrad, ACS Nano, (2019).
[35] C. Tan, S. Pajoumshariati, M. Arshadi, A. Abbaspourrad, Chemical Communications, 55 (2019) 1225-1228.
[36] J. Nogales-Bueno, B. Baca-Bocanegra, A. Rooney, J.M. Hernández-Hierro, H.J. Byrne, F.J. Heredia, Food Chemistry, 232 (2017) 602-609.
[37] M. Fasoli, R. Dell'Anna, S. Dal Santo, R. Balestrini, A. Sanson, M. Pezzotti, F. Monti, S. Zenoni, Plant and Cell Physiology, 57 (2016) 1332-1349.
[38] M. Li, L.-j. Wang, D. Li, Y.-L. Cheng, B. Adhikari, Carbohydrate Polymers, 102 (2014) 136-143.
[39] M. Thiripura Sundari, A. Ramesh, Carbohydrate Polymers, 87 (2012) 1701-1705.
[40] A. Mtibe, L.Z. Linganiso, A.P. Mathew, K. Oksman, M.J. John, R.D. Anandjiwala, Carbohydrate Polymers, 118 (2015) 1-8.
[41] P. Tharra, B. Baire, Chemical Communications, 52 (2016) 14290-14293.
[42] P. Lu, Y.-L. Hsieh, Carbohydrate Polymers, 82 (2010) 329-336.
[43] Y. Shimazaki, Y. Miyazaki, Y. Takezawa, M. Nogi, K. Abe, S. Ifuku, H. Yano, Biomacromolecules, 8 (2007) 2976-2978.
[44] T. Sun, L. Feng, X. Gao, L. Jiang, Accounts of Chemical Research, 38 (2005) 644-652.
[45] M. Liu, Y. Zheng, J. Zhai, L. Jiang, Accounts of Chemical Research, 43 (2010) 368-377.
[46] Y. Wu, J. Feng, H. Gao, X. Feng, L. Jiang, Advanced Materials, 31 (2019) 1800718.
[47] H.-C. Yang, Y. Xie, H. Chan, B. Narayanan, L. Chen, R.Z. Waldman, S.K.R.S. Sankaranarayanan, J.W. Elam, S.B. Darling, ACS Nano, 12 (2018) 8678-8685.
[48] L. Lin, M. Liu, L. Chen, P. Chen, J. Ma, D. Han, L. Jiang, Advanced Materials, 22 (2010) 4826-4830.
[49] J. Li, C. Xu, C. Guo, H. Tian, F. Zha, L. Guo, Journal of Materials Chemistry A, 6 (2018) 223-230.
[50] S. Yuan, J. Zhu, Y. Li, Y. Zhao, J. Li, P. Van Puyvelde, B. Van der Bruggen, Journal of Materials Chemistry A, 7 (2019) 2723-2729.
[51] P.d. calculation.
[52] W. Lv, Q. Mei, J. Xiao, M. Du, Q. Zheng, Advanced Functional Materials, 27 (2017) 1704293.
[53] R. Hönes, J. Rühe, Langmuir, 34 (2018) 5342-5351.
[54] Z. Xue, S. Wang, L. Lin, L. Chen, M. Liu, L. Feng, L. Jiang, Advanced Materials, 23 (2011) 4270-4273.
[55] C. Lee, S. Baik, Carbon, 48 (2010) 2192-2197.
[56] C.P. Whitby, X. Bian, R. Sedev, Colloids and Surfaces A: Physicochemical and Engineering Aspects, 436 (2013) 639-646.
[57] Y.-E. Miao, H.K. Lee, W.S. Chew, I.Y. Phang, T. Liu, X.Y. Ling, Chemical Communications, 50 (2014) 5923-5926.

[58] D. Wang, L. Zhu, J.-F. Chen, L. Dai, Angewandte Chemie International Edition, 55 (2016) 10795-10799.
[59] Z. Liu, Y. Zhang, C. Chen, T. Yang, J. Wang, L. Guo, P. Liu, T. Kong, Small, 15 (2019) 1804549.
[60] N. Raddadi, L. Giacomucci, R. Marasco, D. Daffonchio, A. Cherif, F. Fava, Microbial Cell Factories, 17 (2018) 83.
[61] M. Dandan, H.Y. Erbil, Langmuir, 25 (2009) 8362-8367.